

Tunable spectral shift of high-order harmonic generation in atoms using a sinusoidally phase-modulated pulse

Yue Qiao(乔月), Jun Wang(王俊), Yan Yan(闫妍), Simeng Song(宋思蒙), Zhou Chen(陈洲),Aihua Liu(刘爱华), Jigen Chen(陈基根), Fuming Guo(郭福明), and Yujun Yang(杨玉军)
Citation: Chin. Phys. B, 2022, 31 (**6**): 064214. DOI: 10.1088/1674-1056/ac2d1c
Journal homepage: http://cpb.iphy.ac.cn; http://iopscience.iop.org/cpb

What follows is a list of articles you may be interested in

Orientation and ellipticity dependence of high-order harmonic generation in nanowires

Fan Yang(杨帆), Yinghui Zheng(郑颖辉), Luyao Zhang(张路遥), Xiaochun Ge(葛晓春), and Zhinan Zeng(曾志男)
Chin. Phys. B, 2022, 31 (**4**): 044204. DOI: 10.1088/1674-1056/ac3ed0

Minimum structure of high-harmonic spectrafrom aligned O_2 and N_2 molecules

Bo Yan(闫博), Yi-Chen Wang(王一琛), Qing-Hua Gao(高庆华), Fang-Jing Cheng(程方晶), Qiu-Shuang Jing(景秋霜), Hong-Jing Liang(梁红静), and Ri Ma(马日)
Chin. Phys. B, 2021, 30 (**11**): 114213. DOI: 10.1088/1674-1056/abfbd9

Role of quantum paths in generation of attosecond pulses

M R Sami and A Shahbaz†
Chin. Phys. B, 2020, 29 (**10**): 104207. DOI: 10.1088/1674-1056/ab9deb

An improved method for the investigation of high-order harmonic generation from graphene

Zhong Guan(管仲), Lu Liu(刘璐), Guo-Li Wang(王国利)†, Song-Feng Zhao(赵松峰), Zhi-Hong Jiao(焦志宏), and Xiao-Xin Zhou(周效信)‡
Chin. Phys. B, 2020, 29 (**10**): 104206. DOI: 10.1088/1674-1056/abab76

Resolving multi-orbital effects on high harmonic generation from aligned N_2 molecules in linearly and elliptically polarized intense laser fields

Hong-Jing Liang(梁红静), Xin Fan(范鑫), Shuang Feng(冯爽), Li-Yu Shan(单立宇), Qing-Hua Gao(高庆华), Bo Yan(闫博), Ri Ma(马日), Hai-Feng Xu(徐海峰), Da-Jun Ding(丁大军)
Chin. Phys. B, 2019, 28 (**9**): 094211. DOI: 10.1088/1674-1056/ab3440

Tunable spectral shift of high-order harmonic generation in atoms using a sinusoidally phase-modulated pulse

Yue Qiao(乔月)[1,2], Jun Wang(王俊)[1,†], Yan Yan(闫妍)[1], Simeng Song(宋思蒙)[1], Zhou Chen(陈洲)[1], Aihua Liu(刘爱华)[1], Jigen Chen(陈基根)[2], Fuming Guo(郭福明)[1,‡], and Yujun Yang(杨玉军)[1,§]

[1] *Institute of Atomic and Molecular Physics, Jilin University, Changchun* 130012, *China*
[2] *Department of Physics and Materials Engineering, Taizhou University, Taizhou* 318000, *China*

(Received 13 July 2021; revised manuscript received 9 September 2021; accepted manuscript online 6 October 2021)

High-order harmonic generation (HHG) from an atom illuminated by a sinusoidally phase-modulated pulse is investigated by solving the time-dependent Schrödinger equation. The spectral shift that occurs in atomic HHG can be achieved easily using our laser pulse. It is shown that the photon energy of the generated harmonics is controllable within the range of 1 eV. The shift of the frequency peak position is rooted in the asymmetry of the rising and falling parts of the laser pulse. We also show that by varying the phase parameters in the frequency domain of the laser one can adjust and control the shift in atomic harmonic spectra.

Keywords: high-order harmonic generation, spectra shift

PACS: 42.65.Ky, 98.62.Py **DOI:** 10.1088/1674-1056/ac2d1c

1. Introduction

When atoms and molecules are illuminated by an intense femtosecond laser pulse, electron motion can be modulated periodically and a series of novel physical phenomena arise.[1–6] The rescattering model (collision of the ionized electron with its parent ion in the laser electric field)[7,8] can be used to understand these nonlinear and nonperturbative phenomena of above-threshold ionization as well as high-order harmonic generation (HHG).[9–13] Within low beam divergence[18] and good coherence properties[19] inherited from the driving laser, HHG is the most reliable pathway for producing a coherent light source with spectra from extreme ultraviolet (XUV) to soft x-ray.[20–22] Owing to its wide spectrum, HHG is an important way to produce optical pulses with an attosecond duration.[14–17] HHG can occur in every half cycle of the laser field. According to semiclassical model,[7] high-order harmonic emission occurs through the following three steps: the electron first tunnels through the effective potential barrier formed by the laser field and the atom, then the ionized electron accelerates along the laser electric field, and finally, the electron returns to the parent ion and recombines with the ground state.

As the response of electrons can be affected by the laser field, the process of HHG can be directly initiated using the temporal structure of the laser pulse. In particular, control of the spectral phase of the pulse, and thus its temporal profile, has been demonstrated effectively to give control over numerous physical systems and processes.[23–26] Many theoretical and experimental studies have been carried out to control HHG by modulating the driving laser pulse. For instance, negative frequency chirp atomic HHG is produced by rapidly varying the intensity of ultrashort laser pulses.[27] Several works have focused on the effect of the laser chirp condition on the spectral structure of high-order harmonics emitted from atoms.[27–29] The influence of the carrier envelope phase on a laser-driven dynamic process has been precisely investigated.[30–32] Strobe gating schemes are usually proposed and employed for extending the plateau structure of HHG, such as the polarization gating,[33] amplitude gating,[34] polychromatic laser field[35] and the more complicated double optical gating[36] approaches. Also, the spatial characteristics of inhomogeneous fields and confinement of electron movement play an important role in the HHG process[37–39] and lead to the generation of even harmonics.[39,40]

Given that coherent XUV and x-ray sources are important tools for atomic spectroscopy, characteristics of HHG can be beneficial for applications that require a spectrally tuned single harmonic. Photon energy-tunable XUV radiation is very important in many fields such as spectroscopy,[41] XUV holography[42] and nanolithography.[43] Shaping or tuning the generated harmonics can be achieved by the use of special pulse shapes (e.g., trapezoidal and sine-square like). Oldal *et al*. proposed employing double pulses to generate high-order harmonics with tunable photon energy and spectral width.[44] In other words, the root of spectrally tuned single harmonics is the frequency shift of HHG spectra. Frequency modulation in HHG results from two points: a rapid change envelope effect for ultrashort laser pulses and the propagation ef-

†Corresponding author. E-mail: wangjun86@jlu.edu.cn
‡Corresponding author. E-mail: guofm@jlu.edu.cn
§Corresponding author. E-mail: yangyj@jlu.edu.cn

© 2022 Chinese Physical Society and IOP Publishing Ltd

fect. The propagation effect is negligible if the intensity of the laser pulses and the density of atoms are low. For an instance, Gaussian pulses include a rising and a falling part. In the rising part, compared with the previous cycle, free electrons obtain more kinetic energy from the laser electric field due to the stronger driving force, thus a frequency blueshift appears in the HHG spectra. In the same way, a redshift occurs on the falling part. This frequency chirp has a similar effect to an amplitude chirp.[27] A blueshift in HHG can be achieved easily by using an intense long laser pulse that interacts with atoms and has been extensively studied theoretically.[45–47] A redshift in molecular HHG was studied to probe nuclear motion.[48,49] However, to our knowledge, redshifting in atomic HHG without consideration of the propagation effect has not been reported.

In this paper, we investigate atomic harmonic spectra in the interaction between helium atoms and a sinusoidally phase-modulated laser pulse. Wollenhaupt *et al*. investigated the physical mechanism of strong-field quantum control by shaped femtosecond light fields.[50] We noticed that the frequency domain modulation character of the electric field not only plays an important role leading to a shift in the atomic harmonic spectra but is also a new route for tuning the harmonic central frequency. By simply adjusting the phase parameters in the frequency domain of the incident laser pulses, one can acquire wavelength tuning of the high-order harmonic. This manuscript is organized as follows. Section 2 describes our theoretical model and the numerical method used in this work. In Section 3 the impact of the modulated electric field of laser pulses on spectral modulation in atomic HHG is discussed. Section 4 presents a short summary.

2. Theory

We theoretically investigated the process of HHG from helium atoms in a sinusoidally phase-modulated pulse. The corresponding one-dimensional (1D) time-dependent Schröinger equation (TDSE) in length gauge for this system is written as (unless otherwise stated, atomic units are used throughout this paper)

$$\mathrm{i}\frac{\partial}{\partial t}\psi(x,t)=\left[-\frac{1}{2}\frac{\partial^2}{\partial x^2}+V(x)+E(t)\cdot x\right]\psi(x,t). \tag{1}$$

We solve the 1D TDSE in Eq. (1) by using the split operator scheme;[51] a mask function of the form $\cos^{1/8}$ was employed to avoid unphysical reflection of the wave packet from the boundary. A soft Coulomb function $V(x)=-Z/\sqrt{x^2+a}$ is adopted for the atomic potential function to avoid numerical error caused by the screening potential approaching the origin. With parameters $Z=0.6338$ and $a=0.113$, the corresponding energy of the ground state of helium is -0.9. Then the time-dependent induced dipole moment can be given by Ehrenfest's theorem[52] as follows:

$$\begin{aligned} a(t) &= \frac{\mathrm{d}^2}{\mathrm{d}t^2}\langle\psi(x,t)|x|\psi(x,t)\rangle \\ &= \left\langle\psi(x,t)\left|-\frac{\mathrm{d}V(x)}{\mathrm{d}x}-E(t)\right|\psi(x,t)\right\rangle. \end{aligned} \tag{2}$$

We can obtain the HHG power spectrum $P_a(\omega)$ from the absolute square of the Fourier transformation of the time-dependent dipole accelerations

$$P_a(\omega)=\left|\frac{1}{\omega^2(T-t_0)}\int_{t_0}^{T}a(t)\mathrm{e}^{-\mathrm{i}\omega t}\,\mathrm{d}t\right|^2. \tag{3}$$

We investigated the influence of the total electric field on the HHG process. For a pulse in the linear transform limit, the temporal electric field is expressed as $E(t)=(1/2)E_0f(t)\mathrm{e}^{\mathrm{i}\omega_0 t}+\mathrm{c.c.}$, where E_0 is the peak amplitude of the electric field, $f(t)$ is the envelope of the pulse (assumed to be of Gaussian shape) and ω_0 is the center frequency. Our laser pulse is realized by a simple and intuitive pulse shape parametrization, since the physical mechanism of quantum control using sinusoidal phase modulation in the frequency domain has also been discussed in the time domain,[50] and the properties of the modulated pulses are briefly summarized in the following. As shown in Fig. 1 (upper panel), we start with a transform limit laser pulse $E_{\mathrm{in}}(t)=(1/2)E_0f(t)\mathrm{e}^{\mathrm{i}\omega_0 t}+\mathrm{c.c.}$ The initial electric intensity, full width at half maximum (FWHM) and wavelength of the driving laser pulse are $E_0=0.16$, 10 optical cycles and 800 nm, respectively. Through Fourier transformation, we can obtain $E_{\mathrm{in}}(\omega)$ in the frequency domain. We can modulate the electric field by adding a phase modulation parameter $\widetilde{E}_{\mathrm{out}}(\omega)=\widetilde{E}_{\mathrm{in}}(\omega)\mathrm{e}^{\mathrm{i}\varphi(\omega)}$. In the frequency domain, the phase function is $\varphi(\omega)=A\sin(\omega-\omega_{\mathrm{ref}})T+\phi$, where A describes the amplitude of the phase

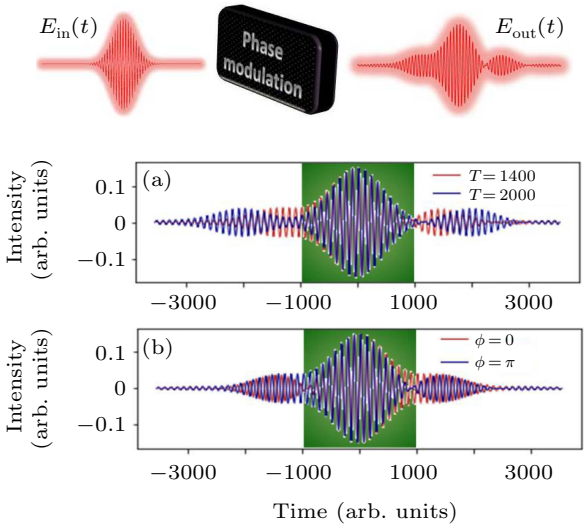


Fig. 1. Temporal evolution of a sinusoidally phase-modulated laser electric field for different frequency phase parameters. All panels are for an intensity of 0.16 and central wavelength of 800 nm. (a) For fixed $\phi=\pi$, the corresponding new envelope for different T [$T=1400$ (solid red line) and $T=2000$ (solid blue line)]. (b) The corresponding temporal amplitude of the new envelope at a fixed $T=1400$ for different absolute phase offsets ϕ.

modulation function, T is the frequency of the sinusoidal oscillation and ϕ is an absolute phase offset, $\omega_{\text{ref}} = 0.057$. Finally, we gain a new temporal envelope function $E_{\text{out}}(t)$ by applying the inverse Fourier transform. The temporal profile of a shaped laser electric field is shown in Figs. 1(a) and 1(b). Figure 1(a) shows how the temporal evolution changes when the frequency of the sinusoidal oscillation $T = 1400$ (solid red line) and $T = 2000$ (solid blue line) and $A = 0.5$ and $\phi = \pi$ are adopted: the symmetry of the pulse shape of laser is broken, especially in green zone, and the pulse in rising part is not equal to that in the falling part. In Fig. 1(b), we fixed $A = 0.5$ and $T = 1400$: when $\phi = 0$ (solid red line) and $\phi = \pi$ (solid blue line), in the time domain, inversion symmetry can be found between them.

3. Results and discussion

We present the harmonic spectra of He atoms irradiated by a sinusoidally phase-modulated pulse with different oscillation frequencies T (Fig. 2). The parameters selected in the calculation are $A = 0.5$, $\phi = \pi$ and $E_0 = 0.16$, with T changing from 1400 to 2000. The harmonic range given in Fig. 2 represents lower-order harmonics (31–35 orders). It can be seen from Fig. 2 that under the driving of a sinusoidally phase-modulated pulse, the harmonic intensities of He atoms under different parameters T are significantly different. The photon energy of the generated harmonics is modulated within the range of 1 eV — a bandwidth comparable to the photon energy of the fundamental field. When the T is small, an obvious redshift from harmonics can be observed. With increase in T, the harmonic peak position gradually moves to the high-energy region and the redshift of the harmonics becomes smaller. However, when T is greater than 1700, the peak position of the harmonics is almost unchanged and the phenomenon of harmonic redshift disappears.

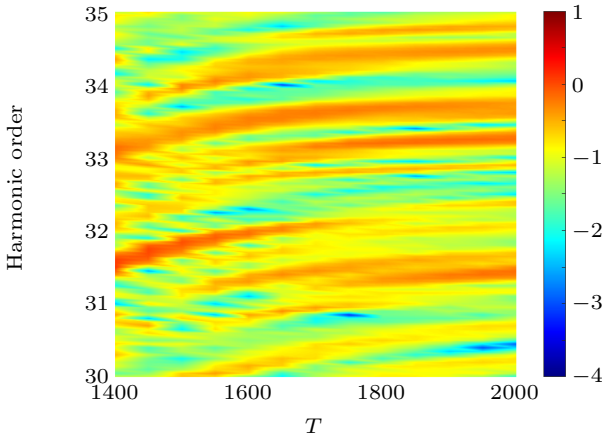


Fig. 2. Variations of the harmonic intensity with different values of the parameter T.

In general, the rising part of the laser field leads to a positive chirp in HHG, where $\mathrm{d}I(t)/\mathrm{d}t > 0$, leading to a blueshift. On the contrary, the falling part of the laser field leads to a negative chirp in HHG, where $\mathrm{d}I(t)/\mathrm{d}t < 0$, leading to a redshift. When the rising and falling parts of the laser are symmetrical, the blueshift and redshift can cancel each other out, and the spectral shift from harmonics cannot be observed. In order to study the phenomenon of harmonic spectral shift for different T values, we present the envelope intensity of the shaped laser electric field when $T = 1400$ (solid red line) and $T = 2000$ (solid blue line) in Fig. 3. The other field parameters are consistent with Fig. 2. As can be seen from Fig. 3, there is a main pulse and two sub-pulses at different T. When $T = 1400$, the distance between the sub-pulses and the main pulse is small, and the first incident sub-pulse will interfere constructively with the main pulse. The overall pulse presents an asymmetrical distribution relative to the intermediate moment. The rising part of the pulse will have a higher intensity than the falling part, resulting in a large change in the harmonic frequency. When $T = 2000$, the sub-pulse gradually moves away from the main pulse, and the overall pulse tends to have a symmetrical structure, so the harmonic peak position hardly changes. Through the above analysis, we know that the parameter T can change the time delay between the main pulse and the sub-pulses of the laser electric field after shaping, thereby changing the overlap of different sub-pulses of the laser electric field and finally giving the laser field an asymmetric structure and shifting the harmonic spectrum. The ionization probability of the shaped pulses with oscillation frequency $T = 1400$ and $T = 2000$ interacting with He atoms is shown in the inset of Fig. 3. By comparing the ionization probability, we find that ionization mainly occurs at the time when the main pulse takes effect; we therefore mainly focus on the effect from the main pulse.

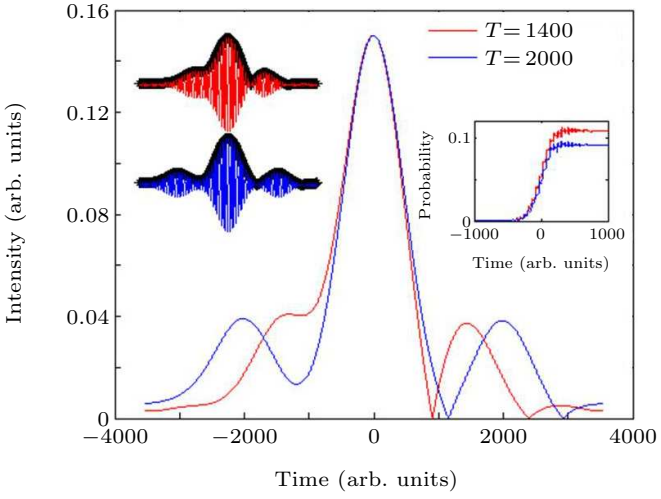


Fig. 3. The envelope intensity of the sinusoidally phase-modulated pulse when $T = 1400$ (solid red line) and $T = 2000$ (solid blue line). The inset shows the ionization probability of an He atom.

In order to further explain the underlying physics of the spectrally shifted HHG from He atoms in the sinusoidally phase-modulated pulse, we also present the derivative of the

main pulse field intensity with respect to time and the asymmetric coefficient under different parameters T in Figs. 4(a) and 4(b). We have previously found that ionization mainly occurs at the time when the main pulse takes effect, so the range given in Fig. 4(a) is −600 to 600. It can be seen that the smaller T is, the greater the degree of asymmetric distribution of the rising and falling parts. When T is larger, the rising and falling parts tend to be symmetrically distributed. We define the asymmetry coefficient between the rising part and the falling part as $S = \frac{|\max(\mathrm{d}I(t)/\mathrm{d}t)|-|\min(\mathrm{d}I(t)/\mathrm{d}t)|}{|\max(\mathrm{d}I(t)/\mathrm{d}t)|}$. The asymmetric coefficient as a function of the frequency of the sinusoidal oscillation is shown in Fig. 4(b). It is found through calculation that when $T = 1400$, the asymmetry coefficient is −0.1122. When $T = 2000$, the asymmetry coefficient is −0.001. As T increases, the asymmetry coefficient of the rising and falling parts of the laser field becomes smaller. Furthermore, in Fig. 4(c) we compare the change in the harmonic spectrum with T with the fitting curve of the asymmetry coefficient. The relationship between harmonic shift and the asymmetry coefficient is given by $K = \frac{||q_{T=2000}|-|q_{T=1400}||}{||S_{T=2000}|-|S_{T=1400}||}$, where q is the harmonic order. As long as the asymmetric coefficient of the pulse is known, the energy shift range of the harmonics can be found. Here we only display the fitting curve when $q_{T=1400} = 33.1$th and $q_{T=2000} = 33.75$th. From the above formula, $K = 5.85$. The fitting curve of the asymmetry coefficient is indicated by the red circle. We can also see that the change trend of the harmonic intensity with T is consistent with the change trend of the asymmetry coefficient with T. The shift of the harmonic spectrum is related to the asymmetry coefficient. This further confirms our view.

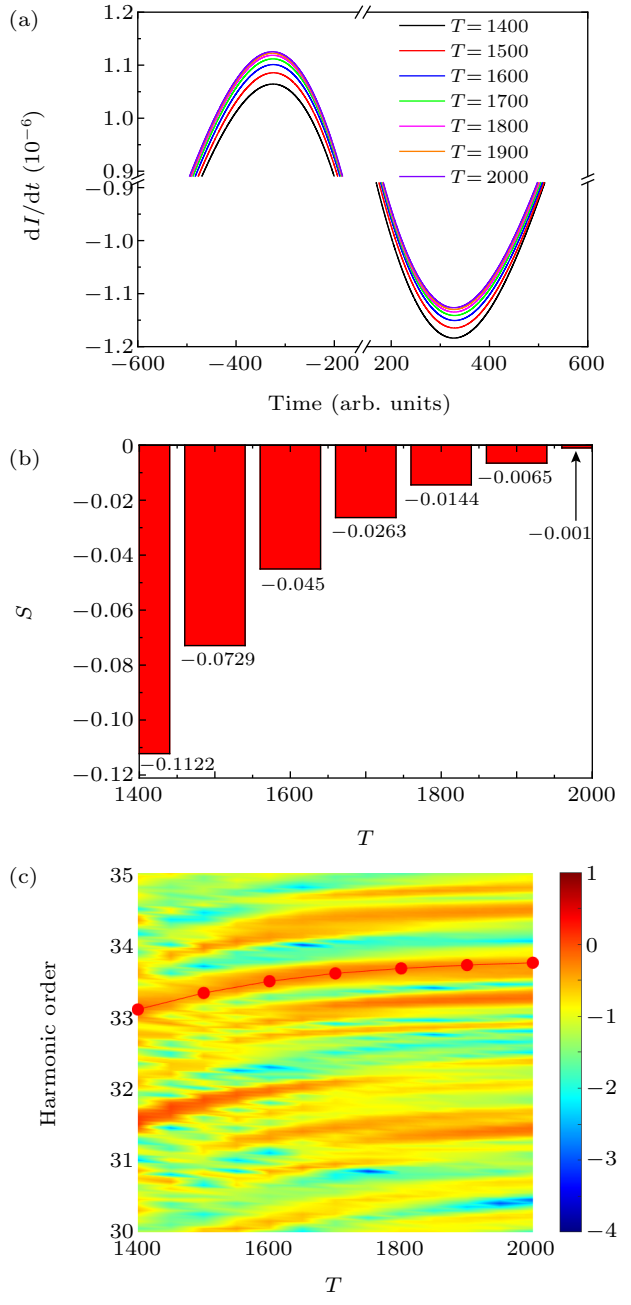


Fig. 4. (a) The derivative of intensity versus time and (b) the asymmetric coefficient as a function of the oscillation frequency T. (c) Comparison of the harmonic spectrum and the asymmetry coefficient.

The harmonic intensity is affected not only by the oscillation frequency T but also by the absolute phase offset ϕ. Figure 5(a) shows the harmonic spectra of He atoms as a function of ϕ. The parameters selected in Fig. 5(a) are $A = 0.5$, $T = 1400$, and $E_0 = 0.16$, while ϕ changes from 0 to 2π. We can see from Fig. 5(a) that the emission intensity of the 40–45th order harmonics has an oscillating structure with change of ϕ. Under the modulation of ϕ, the peak of the harmonic spectrum moves significantly. In the process of changing from 0 to π, the peak of the harmonic moves to a low-energy region, and in the process of changing from π to 2π, the peak of the harmonic moves to a high-energy region. This is because the phase offset can be changed by ϕ, and the phase difference between the sub-pulse and the main pulse can be changed without changing the amplitude of the main pulse and the sub-pulse, as shown in Fig. 5(b). When $\phi = 0$, the rising part changes faster than the falling part, where $\mathrm{d}I(t)/\mathrm{d}t > 0$, leading to a blueshift. On the country, the falling part changes faster than the rising part when $\phi = \pi$, where $\mathrm{d}I(t)/\mathrm{d}t < 0$, leading to a redshift. In this way, the asymmetry of the rising and falling parts of the laser pulse is adjusted, and the frequency peak position of the harmonic emission is adjusted. The asymmetric coefficient as a function of the absolute phase offset ϕ is shown in Fig. 5(c). We can see that the asymmetry coefficient shows a symmetrical structure relative to $\phi = \pi$. During the change from 0 to π, the asymmetry coefficient changes from positive to negative and harmonics change from blueshift to redshift, so the peak of the harmonic moves to a low-energy region. During the change from 0 to 2π, the asymmetry coefficient changes from negative to positive and harmonics change from redshift to blueshift, so the peak of the harmonic moves to a high-energy region.

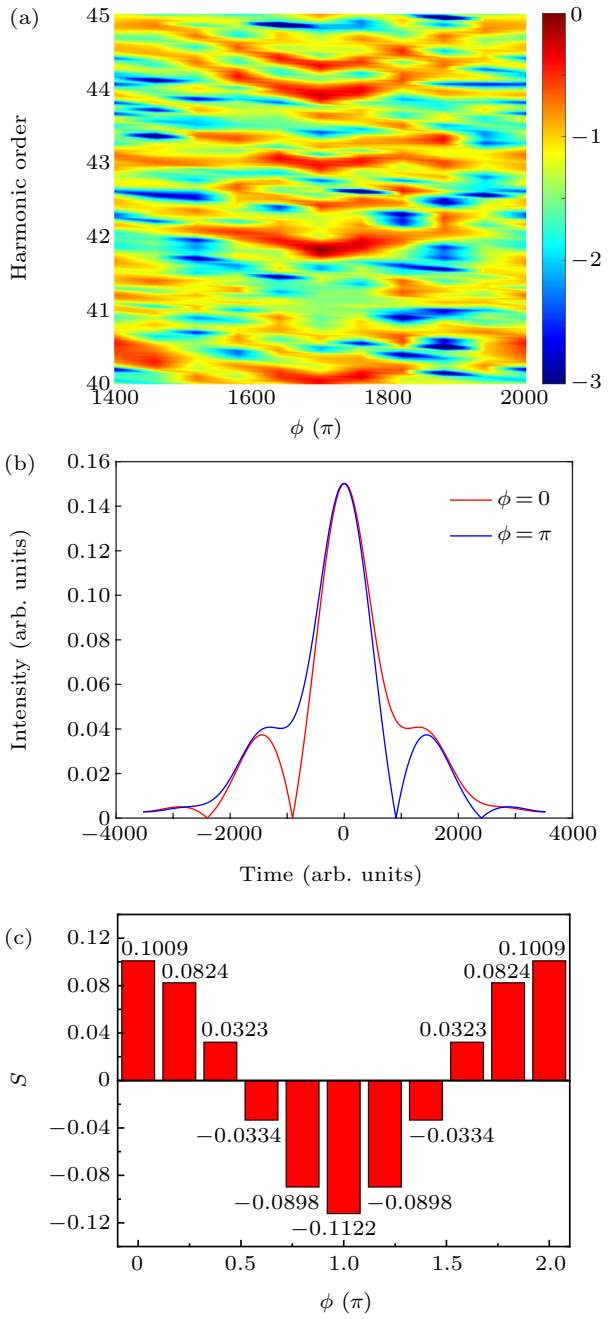


Fig. 5. (a) Harmonic intensity as a function of the parameter ϕ. (b) The envelope intensity of the sinusoidally phase-modulated pulse when $\phi = 0$ (solid red line) and $\phi = \pi$ (solid blue line). (c) The asymmetry coefficient as a function of the absolute phase offset ϕ.

4. Conclusions and final remarks

The frequency modulation of atomic high-order harmonics by a sinusoidally phase-modulated pulse is investigated theoretically. We have numerically solved the one-dimensional TDSE based on a single active-electron model. It is found that the spectral shift of a high-order harmonic can be observed when the symmetry of the pulse shape of the laser is broken. The shape of our pulse in the rising part is not equal to that in the falling part. The rising part of the laser field leads to a positive chirp in HHG, where $\mathrm{d}I(t)/\mathrm{d}t > 0$, leading to a blueshift. On the country, the falling part of the laser field leads to a negative chirp in HHG, where $\mathrm{d}I(t)/\mathrm{d}t < 0$, leading to a redshift. The asymmetry coefficient S between the rising and falling parts is shown: as T increases, S becomes smaller. The shift in the frequency peak position decreases gradually. Our procedure gives the possibility of tuning the central wavelength of the driving source itself. Spectral shifting of high-order harmonics is observed due to the failure to balance between the blueshift and the redshift. This shift in atomic harmonic spectra can be controlled by changing the phase parameters in the frequency domain. Tunable high-order harmonics should also prove useful as a seeding pulse for x-ray lasers. We predict that in the near future a spectral shift can be observed by means of this scheme using propagation effects.

Acknowledgments

Project supported by the National Natural Science Foundation of China (Grant Nos. 11604119, 11627807, 11774129, 11774131, 11904120, 11975012, and 91850114) and the Outstanding Youth Project of Taizhou University (Grant No. 2019JQ002).

References

[1] Li F, Yang Y J, Chen J, Liu X J, Wei Z Y and Wang B B 2020 *Chin. Phys. Lett.* **37** 113201
[2] Li W K, Lei Y, Li X, Yang T, Du M, Jiang Y, Li J L, Lou S Z, Liu A H, He L H, Ma P, Zhang D D and Ding D J 2021 *Chin. Phys. Lett.* **38** 053202
[3] Yang W F, Li J, Jia W B, Zhang H D, Liu X W, Zhu M, Song X H and Chen J 2021 *Phys. Rev. A* **103** 053105
[4] Yang W F, Song X H, Gong S Q, Cheng Y and Xu Z Z 2007 *Phy. Rev. Lett.* **99** 133602
[5] Liu X W, Zhang G J, Li J, Shi G L, Zhou M Y, Song X H and Yang W F 2020 *Phy. Rev. Lett.* **124** 113202
[6] Song X H, Shi G L, Zhang G J, Xu J W, Lin C, Chen J and Yang W F 2018 *Phy. Rev. Lett.* **121** 103201
[7] Corkum P B 1993 *Phy. Rev. Lett.* **71** 1994
[8] Lewenstein M, Balcou Ph, Ivanov M Yu, L'Huillier A and Corkum P B 1994 *Phys. Rev. A* **49** 2117
[9] Zhao Y T, Ma S Y, Jiang S C, Yang Y J, Zhao X and Chen J G 2019 *Opt. Express* **27** 34392
[10] Zhao Y T, Xu X Q, Jiang S C, Zhao X, Chen J G and Yang Y J 2020 *Phys. Rev. A* **101** 033413
[11] Zhao Y T, Jiang S C, Zhao X, Chen J G and Yang Y J 2020 *Opt. Lett.* **45** 2874
[12] Jin C, Wang S J, Zhao X, Zhao S F, Wang S J and Lin C D 2020 *Phys. Rev. A* **101** 013429
[13] Zhang H D, Liu X W, Jin F C, Zhu M, Yang S D, Dong W H, Song X H and Yang W F 2021 *Chin. Phys. Lett.* **38** 063201
[14] Wang X W, Wang L, Xiao F, Zhang D W, Lu J M, Yuan J M and Zhao Z X 2020 *Chin. Phys. Lett.* **37** 023201
[15] Zhao X, Wang S J, Yu W W, Wei H, Wei C L, Wang B C, Chen J G and Lin C D 2020 *Phys. Rev. Appl.* **13** 034043
[16] Zhao X, Wei H, Wu Y and Lin C D 2017 *Phys. Rev. A* **95** 043407
[17] Zhao X, Wang S J, Wang B C and Lin C D 2020 *J. Phys. B: At. Mol. Opt. Phys.* **53** 154002
[18] Lee D G, Kim H T, Hong K H, Nam C H, Choi I W, Bartnik A and Fiedorowicz H 2002 *Appl. Phys. Lett.* **81** 3726
[19] Bellini M, Lyngå C, Tozzi A, Gaarde M B, Hänsch T W, L'Huillier A and Wahlström C G 1998 *Phy. Rev. Lett.* **81** 297
[20] Burnett N H, Baldis H A, Richardson M C and Enright G D 1977 *Appl. Phys. Lett.* **31** 172

[21] Brabec T and Krausz F 2000 *Rev. Mod. Phys.* **72** 545
[22] Hentschel M, Kienberger R, Spielmann C, Reider G A, Milosevic N, Brabec T, Corkum P, Heinzmann U, Drescher M and Krausz F 2001 *Nature* **414** 509
[23] Assion A, Baumert T, Bergt M, Brixner T, Kiefer B, Seyfried V, Strehle M and Gerber G 1998 *Science* **282** 919
[24] Bartels R, Backus S, Zeek E, Misoguti L, Vdovin G, Christov I P, Murnane M M and Kapteyn H C 2000 *Nature* **406** 164
[25] Weinacht T C, Ahn J and Bucksbaum P H 1999 *Nature* **397** 233
[26] Zhao X Y, Wang C C, Hu S L, Li W D, Chen J and Hao X L 2019 *Chin. Phys. B* **28** 83202
[27] Chang Z, Rundquist A, Wang H, Christov I, Kapteyn H C and Murnane M M 1998 *Phys. Rev. A* **58** R30
[28] Lee D G, Kim J H, Hong K H and Nam C H 2001 *Phy. Rev. Lett.* **87** 243902
[29] Sekikawa T, Ohno T, Yamazaki T, Nabekawa Y and Watanabe S 1999 *Phy. Rev. Lett.* **83** 2564
[30] de Bohan A, Antoine P, MiloŠević D B and Piraux B 1998 *Phy. Rev. Lett.* **81** 1837
[31] Sansone G, Vozzi C, Stagira S, Pascolini M, Poletto L, Villoresi P, Tondello G, de Silvestri S and Nisoli M 2004 *Phy. Rev. Lett.* **92** 113904
[32] Zhao X, Chen J, Fu P, Liu X, Yan Z C and Wang B 2013 *Phys. Rev. A* **87** 043411
[33] Corkum P B, Burnett N H and Ivanov M Y 1994 *Opt. Lett.* **19** 1870
[34] Goulielmakis E, Schultze M, Hofstetter M, Yakovlev V S, Gagnon J, Uiberacker M, Aquila A L, Gullikson E M, Attwood D T, Kienberger R, Krausz F and Kleineberg U 2008 *Science* **320** 1614
[35] Chen J G, Yang Y J, Zeng S L and Liang H Q 2011 *Phys. Rev. A* **83** 023401
[36] Mashiko H, Gilbertson S, Li C, Khan S D, Shakya M M, Moon E and Chang Z 2008 *Phy. Rev. Lett.* **100** 103906
[37] Wang J, Chen G, Li S Y, Ding D J, Chen J G, Guo F M and Yang Y J 2015 *Phys. Rev. A* **92** 033848
[38] Han J X, Wang J, Qiao Y, Liu A H, Guo F M and Yang Y J 2019 *Opt. Express* **27** 8768
[39] Ciappina M F, Biegert J, Quidant R and Lewenstein M 2012 *Phys. Rev. A* **85** 033828
[40] Guo Y, Liu A H, Wang J and Liu X S 2019 *Chin. Phys. B* **28** 094212
[41] Cingöz A, Yost D C, Allison T K, Ruehl A, Fermann M E, Hartl I and Ye J 2012 *Nature* **482** 68
[42] Bartels R A, Paul A, Green H, Kapteyn H C, Murnane M M, Backus S, Christov I P, Liu Y, Attwood D and Jacobsen C 2002 *Science* **297** 376
[43] Solak H H 2006 *J. Phys. D: Appl. Phys.* **39** R171
[44] Gulyás Oldal L, Csizmadia T, Ye P, Harshitha N G, ZaÏr A, Kahaly S, Varjú K, Füle M and Major B 2020 *Phys. Rev. A* **102** 013504
[45] Watson J B, Sanpera A and Burnett K 1995 *Phys. Rev. A* **51** 1458
[46] Schafer K J and Kulander K C 1997 *Phy. Rev. Lett.* **78** 638
[47] Geissler M, Tempea G and Brabec T. 2000 *Phys. Rev. A* **62** 033817
[48] Bian X B and Bandrauk A D. 2014 *Phy. Rev. Lett.* **113** 193901
[49] Du H, Xue S, Wang H, Zhang Z and Hu B 2015 *Phys. Rev. A* **91** 063844
[50] Wollenhaupt M, Präkelt A, Sarpe-Tudoran C, Liese D, Bayer T and Baumert T 2006 *Phys. Rev. A* **73** 063409
[51] Yang Y J, Chen J G, Chi F P, Zhu Q R, Zhang H X and Sun J Z 2007 *Chin. Phys. Lett.* **24** 1537
[52] Wang J, Chen G, Guo F M, Li S Y, Chen J G and Yang Y J 2013 *Chin. Phys. B* **22** 033203